Journal of
Applied Research in Water and Wastewater
Journal homepage: www.arww.razi.ac.ir

Original paper

A TVD-WAF finite volume model for roll wave simulation

Ali Mahdavi

Department of Civil Engineering, Arak University, Arak, Iran.

ARTICLE INFO

Article history:
Received 25 June 2016
Received in revised form 31 July 2016
Accepted 14 August 2016

Keywords:
Roll waves
Numerical method
WAF scheme
Steep channel

ABSTRACT

Roll waves appear as successive transitions from super- to sub-critical flows by passing through moving hydraulic jumps. Such discontinuous periodic waves propagate in a staircase pattern at constant wave celerity. On the basis of nonlinear shallow water (NLSW) equations, a finite volume model is presented to study the evolution of roll waves in inclined steep channels. The numerical model exploits the total variation diminishing version of weighted average flux (TVD-WAF) explicit method to solve the homogeneous NLSW equations. An implicit trapezoidal time integration operator is implemented for the treatment of source term which includes contributions from both the channel slope and frictional resistance. The simulated surface profile and flow velocity are in well agreement with available analytical solution for roll waves. The time evolution of wave amplitude under different undisturbed Froude numbers are investigated numerically and compared with theoretical predictions. Temporal decay of initial disturbance is discussed in which case roll waves no longer form. The observed agreement implies the efficiency and accuracy of the present scheme for roll wave modeling.

1. Introduction

Considering a steady uniform flow down an inclined steep channel with bed friction, once the Froude number exceeds a definite critical value, the flow reveals some sort of hydrodynamic unstability and the disturbances on the free surface, if exist, may eventually grow forming a series of successive hydraulic bores connected by smooth profiles of gradually varied flow. Such discontinuous periodic waves propagate in a staircase pattern at constant wave celerity and are known as roll waves.

From practical point of view, it is important to consider the role of roll waves in the design of channels, since these water carrying structures may be overtopped by formation of roll waves (Montes. 1998). Dressler (1949) was the first who mathematically explained the occurrence of periodic roll waves in an open channel of constant slope and obtained a quasi-steady solution for roll waves. He assumed a uniformly moving frame of reference to formulate traveling waves. The critical value of Froude number to onset instabilities was found to be F_0=2 based on mathematical analysis of linearized theory where a small perturbation is being imposed on a steady uniform state (Whitham. 1974; Que and Xu. 2006). This threshold condition for the formation of roll waves has been also confirmed by experiments (Brock. 1967).

In addition to man-made canals such as draining systems and dam spillways, roll waves have also been observed in natural water courses such as ice channels (Carver, Sear and Valentine. 1999) and lakes (Fer, Lemmin and Thorpe. 2003). Balmforth and Mandre (2004) reported disturbances in a variety of physical situations that behaves, in some aspects, similar to roll waves in open channel flows. These include perturbations in multi-phase fluid, mudflow, granular layers and flow down collapsible tubes and elastic conduits. It is worth mentioning that the phenomenon of roll wave is precisely analogous to the stop-start waves encountered in freeway models of traffic theory (Kühne. 1984).

The nonlinear shallow water (NLSW) equations have been broadly accepted for modeling long wave evolution in open channels as well as coastal areas (Mahdavi and Talebbeydokhti. 2009, 2011; Mahdavi et al. 2012). The hyperbolic nature of this system of partial differential equations admits discontinuous solutions (e.g., hydraulic jump, bore, breaking wave and roll wave) even when the initial conditions are spatially smooth. Based on the one dimensional NLSW, Zanuttigh and Lamberti (2002) found satisfactory results in reproducing the Brock's experimental roll waves in a laboratory flume. The same authors further studied the stability of viscoplastic fluid in uniform flow, proving that debris flows become unstable even for F_0<1 (Zanuttigh and Lamberti. 2004). Di Cristo et al. (2008) established a formula on the minimum channel length required for roll wave development. Their results were found reliable when compared to available experimental data, regardless of the channel slope. Que and Xu (2006) developed a high resolution scheme based on the gas-kinetic Bhatnagar–Gross–Krook (BGK) model to study roll-waves down an inclined open channel.

In the present study, the generation and propagation of roll waves are numerically investigated in the framework of an initial value problem for NLSW equations. The TVD-WAF scheme is considered as an approximate Riemann solver to provide the model with shock capturing property in presence of discontinuities across the front of roll waves and to allow the formation of smooth segments of gradually varied flow linking each two consecutive bore faces. The accuracy of the scheme is verified through comparisons with the available analytical solution and with the numerical results obtained by the BGK kinetic scheme of Que and Xu (2006).

2. Materials and methods

Governing equations

Referring to the definition sketch (Fig. 1), the generation and evolution of roll waves are considered here. The relevant process can be appropriately described by the non-linear shallow water equations written in the conservative form as:

$$\frac{\partial \mathbf{U}}{\partial t}+\frac{\partial \mathbf{F}}{\partial x}=\mathbf{S} \qquad (1)$$

Corresponding author Email: a-mahdavi@araku.ac.ir

The conserved variables U, the flux F, and the source term S are defined respectively by:

$$\mathbf{U}=\begin{bmatrix} h \\ hu \end{bmatrix},\quad \mathbf{F}(\mathbf{U})=\begin{bmatrix} hu \\ hu^2+\frac{1}{2}gh^2 \end{bmatrix},\quad \mathbf{S}(\mathbf{U})=\begin{bmatrix} 0 \\ ghS_o-C_f u^2 \end{bmatrix}. \tag{2}$$

In the above equations, t denotes time, x is the distance along the channel, h (x, t) is the water depth, u (x, t) is the depth-averaged velocity along x-direction, C_f is the bed roughness coefficient, S_o is the bottom slope and g is the gravitational acceleration.

In the context of numerical schemes, it is usual to approximate the spatial derivative of non-linear flux F in Eq. (1) at x_i (the center of cell *i*) by the conservative difference as:

$$\left(\frac{\partial \mathbf{F}}{\partial x}\right)_{x=x_i}=\frac{\mathbf{F}_{i+1/2}-\mathbf{F}_{i-1/2}}{\Delta x} \tag{3}$$

where Δx is the spatial cell size and $F_{i+1/2}$ and $F_{i-1/2}$ are the inter-cell numerical fluxes that will be explained in the next paragraphs.

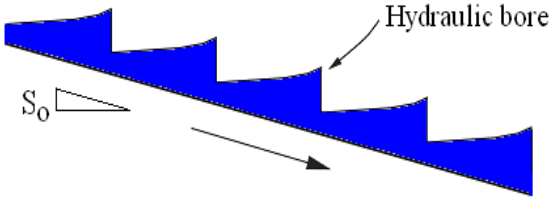

Fig. 1. Definition sketch for propagation of roll waves.

Evaluation of numerical flux

To precisely handle the shock-like wave front of roll waves, the inter-cell numerical fluxes are computed by the weighted average flux (WAF) shock capturing method. A limiter function enforces the total variation diminishing (TVD) constraint on the scheme and, thereby, adding sufficient dissipation to the scheme to ensure the monotonicity near large gradients of the solution. The TVD-WAF scheme preserves second order accuracy in spatial and temporal coordinates and is oscillation-free across discontinuities. The numerical flux may be written as (Toro. 2001):

$$\mathbf{F}_{i+1/2}=\frac{1}{2}(\mathbf{F}_i+\mathbf{F}_{i+1})-\frac{1}{2}\sum_{k=1}^{N}\mathrm{sign}(c_k)\phi_{i+1/2}^{(k)}\Delta\mathbf{F}_{i+1/2}^{(k)} \tag{4}$$

where N denotes the number of waves in the solution of Riemann problem, $\Delta\mathbf{F}_{i+1/2}^{(k)}=\mathbf{F}_{i+1/2}^{(k+1)}-\mathbf{F}_{i+1/2}^{(k)}$ is the flux jump across wave k with fluxes defined by $\mathbf{F}_{i+1/2}^{(1)}=\mathbf{F}(\mathbf{U}_L)$, $\mathbf{F}_{i+1/2}^{(2)}=\mathbf{F}(\mathbf{U}^*)$ and $\mathbf{F}_{i+1/2}^{(3)}=\mathbf{F}(\mathbf{U}_R)$, c_k is the Courant number for wave k and $\phi_{i+1/2}^{(k)}$ is the limiter function. Some suitable choices for limiter function are reported by Toro (2001). The SUPERBEE limiter is preferred for the present applications. It is given by:

$$\phi_{i+1/2}^{(k)}=1-\left(1-|c_k|\right).\max\left[0,\ \min\left(1,\ 2r^{(k)}\right),\ \min\left(2,\ r^{(k)}\right)\right] \tag{5}$$

where $r^{(k)}$ is the ratio of the upwind change to the local change in flow depth for which the details can be found in Toro(2001). In (4), the numerical flux $\mathbf{F}_{i+1/2}^{(2)}=\mathbf{F}(\mathbf{U}^*)$ refers to the Harten-Lax-van Leer (HLL) approximate Riemann solver. Based on the HLL approach, the Riemann problem with data U_L and U_R is characterized by three constant states separated by two waves. The numerical flux in the intermediate region of the wave structure can be determined as follows:

$$\mathbf{F}(\mathbf{U}^*)=\frac{S_R\mathbf{F}(\mathbf{U}_L)-S_L\mathbf{F}(\mathbf{U}_R)+S_RS_L(\mathbf{U}_R-\mathbf{U}_L)}{S_R-S_L} \tag{6}$$

where S_L and S_R represent the wave speed estimates on the left and right sides of the cell interface, respectively. Several options are available for these wave speeds. The wave speed expressions derived by Toro (1992) is implemented in the present model:

$$\begin{aligned} S_R&=\max(u_R+\sqrt{gh_R},u^*+\sqrt{gh^*}) \\ S_L&=\min(u_L-\sqrt{gh_L},u^*-\sqrt{gh^*}) \end{aligned} \tag{7}$$

In above expressions $h^*$and u^*denote, respectively, the flow depth and flow velocity in the intermediate region of the wave structure. According to the two-rarefaction approach, these flow variables can be evaluated by the following closed-form solutions:

$$\begin{aligned} h^*&=\frac{1}{g}\left[\frac{1}{2}(\sqrt{gh_L}+\sqrt{gh_R})+\frac{1}{4}(u_L-u_R)\right]^2 \\ u^*&=\frac{1}{2}(u_L+u_R)+\sqrt{gh_L}-\sqrt{gh_R} \end{aligned} \tag{8}$$

Treatment of source term

A numerical procedure for dealing with the homogeneous NLSW equations was explained in foregoing section. In presence of source term, the TVD-WAF scheme can be applied unchanged, if the source term is treated by additional integration steps. To this end, a three step splitting scheme is implemented that relies on successive solution of following system of initial value sub-problems.

$$\begin{aligned} &\text{ODEs:}\quad \frac{\mathrm{d}\mathbf{U}}{\mathrm{d}t}=\mathbf{S}(\mathbf{U}) \\ &\text{ICs:}\quad \mathbf{U}^n \end{aligned} \Bigg\} \xrightarrow{\Delta t'} \mathbf{U}^{(1)}$$

$$\begin{aligned} &\text{PDEs:}\quad \frac{\partial \mathbf{U}}{\partial t}+\frac{\partial \mathbf{F}}{\partial x}=\mathbf{0} \\ &\text{ICs:}\quad \mathbf{U}^{(1)} \end{aligned} \Bigg\} \xrightarrow{\Delta t} \mathbf{U}^{(2)} \tag{9}$$

$$\begin{aligned} &\text{ODEs:}\quad \frac{\mathrm{d}\mathbf{U}}{\mathrm{d}t}=\mathbf{S}(\mathbf{U}) \\ &\text{ICs:}\quad \mathbf{U}^{(2)} \end{aligned} \Bigg\} \xrightarrow{\Delta t'} \mathbf{U}^{n+1}$$

where superscript n denotes the current time level, Δt is the time step size and Δt′=Δt/2. In present work, the source term parts are treated by the trapezoidal time integration method. This implicit operator is second-order accurate and can be expressed for the first sub-problem in Eq. (9) as:

$$\left[\mathbf{I}-\frac{\Delta t'}{2}\left(\frac{\partial \mathbf{S}(\mathbf{U})}{\partial \mathbf{U}}\right)_i^n\right]\Delta\mathbf{U}_i=\Delta t'\mathbf{S}(\mathbf{U}_i^n) \tag{10}$$

where I denotes the identity matrix and $\Delta U_i = U_i^{(1)}–U_i^n$ is the temporal jump in conserved variables. The second term of the right-hand side of Eq. (10) is the Jacobian matrix of the source term. The first intermediate value $U^{(1)}$ can be calculated from Eq. (10). Taking $U^{(2)}$ as the initial condition, the TVD-WAF scheme is then implemented in an explicit conservative scheme to obtain the second intermediate value $\mathbf{U}^{(2)}$ as:

$$\mathbf{U}^{(2)}=\mathbf{U}^{(1)}-\frac{\Delta t}{\Delta x}(\mathbf{F}_{i+1/2}-\mathbf{F}_{i-1/2}) \tag{11}$$

The above conservative formula results from integrating the homogeneous NLSW equations over a suitable control volume in the x-t plane. Finally, applying the source term operator to $U^{(2)}$ will give the conserved variables at the new time level, n+1. Because the TVD-WAF is an explicit scheme, the magnitude of time interval Δt is dynamically adjusted according to the Courant- Friedrichs-Lewy (CFL) criterion, defined as:

Please cite this article as: A. Mahdavi, A TVD-WAF finite volume model for roll wave simulation, Journal of Applied Research in Water and Wastewater, 3 (2), 2016, 241-246.

$$\Delta t = C_n \min_i \frac{\Delta x}{|u_i| + \sqrt{g h_i}} \quad (12)$$

with C_n being the CFL number ($0 < C_n \leq 1$).

Initial and boundary conditions

In order to constitute a mathematically well-posed problem, it is necessary to prescribe the initial and boundary conditions that are consistent with the true behavior of the physical phenomenon under consideration. To specify the initial conditions for modeling roll waves, the approach proposed by Que and Xu (2006) is followed which provides a simple and robust procedure to model the generation and subsequent evolution of roll waves. According to their formulation, the initial sinusoidal disturbance and corresponding initial flow velocity are respectively designated by:

$$h(x,0) = h_0\left[1 + \varepsilon \sin(k_w x)\right]$$
$$u(x,0) = u_0 + r_p \varepsilon \sin(k_w x + \theta_p) \quad (13)$$

In the above equations, ε is an amplification factor accounting for the amplitude of the initial disturbance which was suggested to be ε=0.005 in the original paper, k_w is the 2π-wave number, h_0 and u_0 are the water depth and flow velocity of the undisturbed initial flow, respectively. θ_p is the phase lag between the initial water depth and associated flow velocity and r_p represents a function of angular velocity, wave number and initial flow velocity for which an expression was introduced by Que and Xu (2006). The existence of initial uniform flow down a sloping channel requires a situation in which the gravitational and frictional forces approach equilibrium such that:

$$S_o = C_f F_0^2 \quad (14)$$

where $F_0 = u_0/(gh_0)^{1/2}$ is the Froude number of initial undisturbed flow and the variables with subscript 0 refer to those associated with initial uniform flow. The adoption of periodic boundary condition at either ends of the computational domain enables efficient representation of the periodic properties of roll waves. This type of boundary condition simultaneously equates the conserved variables at two boundaries of the model.

3. Results and discussion

The numerical values of the physical parameters adopted herein mostly follow those of Que and Xu (2006). Fig. 2 shows the snapshots of depth profiles for a uniform flow ($q_0=h_0u_0$=0.001 $m^2 s^{-1}$, F_0 =2.5) primarily disturbed by imposing a sinusoidal perturbation (k_w=10π and ε=0.005) over its free surface. The flow domain has a length of 2 m (0<x<2m) and is discretized by 1000 computational cells (Δx=0.002 m). The numerical stability of the roll wave simulation is guaranteed by setting C_n = 0.65. The bed friction is included in the computation by a roughness coefficient of C_f=0.006 and the channel slope is S_o=0.0375 as determined by Eq. (14). Obviously, the amplitude of initial disturbance grows up with time until a permanent form wave is established around t=20s. At this stage, the wave train experiences successive transitions from super- to sub-critical flows through moving hydraulic jumps. This situation is shown in Fig. 3. The moving reference Froude number is defined as $F_{mr} = (c-u)/\sqrt{gh}$ with c being the constant wave celerity which is evaluated as $c = 0.55\,\mathrm{ms}^{-1}$ in this case. This definition is equivalent to an observer moving with roll wave for which the wave appears to be stationary. In this manner, the problem may be simplified to steady-flow formation of hydraulic jumps. It can be seen that the difference between the maximum F_{mr} and minimum F_{mr} increases by increasing F_0 (Fig. 4). These maximum and minimum Froude numbers correspond to conjugate depths associated with moving hydraulic jumps. An increase of F_0 obviously leads to greater maximum F_{mr} which in turn increases the specific force before jump. Therefore, the specific force after the jump should also grow to maintain the balance between the specific forces acting on either sides of the jump (taking into account the bottom friction force). The threshold Froude number F_0 = 2 implies the dominance of critical flow regime throughout the domain which is indicated by F_{mr} = 1 in Fig. 4.

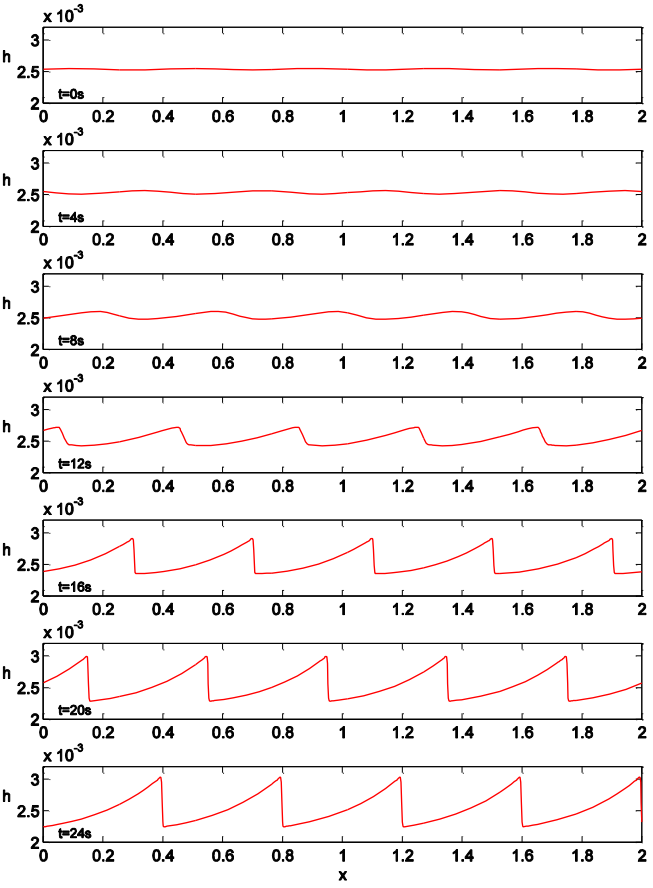

Fig. 2. Snapshots of depth profiles representing the generation and evaluation of roll waves at different times. The channel has a length of 2m; the steady state flow is designated by: q_0 = 0.001 m^2S^{-1}, F_0 = 2.5, C_f = 0.006; and the initial disturbance takes these parameter values: $k_w = 10\pi$ and $\varepsilon = 0.005$ (The axes are in meter).

In Fig. 5, depth and velocity profiles of emerged roll waves are checked against the analytical solution of Dressler (1949). The agreement is quite satisfactory in terms of predicting the locations of bore faces and simulating the smooth connecting profiles. The time history of flow variables at the middle of the channel i.e., x=1m are depicted in Fig. 6 along with the results obtained by a high resolution BGK kinetic scheme developed by Que and Xu (2006). The results of these two models reveal a similar pattern for both amplitude growth and temporal variation of flow velocity at this location.

Lukáčová-Medviďová and Teschke (2006), performing a comparison study of various numerical shallow water models, noted that the CPU-efficiency needs to be considered relatively since it depends on the optimality and robustness of a code. Therefore, comparisons are also made between simulation run times of the two models. In the cases studied, it was found that the CPU time consumed by the TVD-WAF scheme is only about 30−33 % of that needed by the BGK scheme, implying the efficiency of the present model with respect to its CPU performance.

The natural logarithm of maximum wave amplitude as a function of time under several Froude numbers ranging from F_0=1.5 to F_0=3.7 is presented in Fig. 7. Also depicted in this figure are the linear theory predictions (Que and Xu, 2006). At the first stages of wave evolution, the amplitude growth rate is in agreement with theoretical results obtained by the linear theory, but as time continues, the wave amplitude is no longer small and the wave form undergoes a change towards successive hydraulic bores leading to appearance of nonlinear effects and thus divergence from linear theory. However, the validity range of linear theory tends to extend when the Froude number of initial flow is reduced.

Please cite this article as: A. Mahdavi, A TVD-WAF finite volume model for roll wave simulation, Journal of Applied Research in Water and Wastewater, 3 (2), 2016, 241-246.

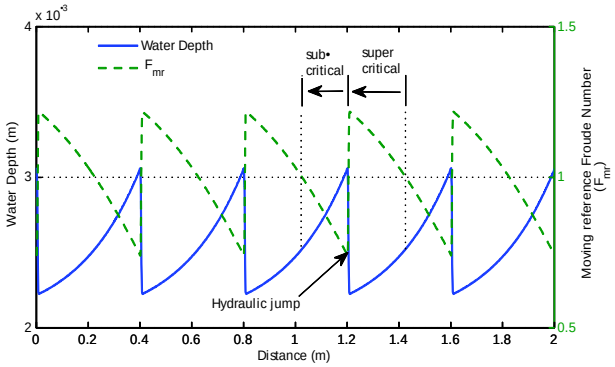

Fig. 3. Transition from super- to sub-critical flow regimes in roll waves. The waves propagate toward right.

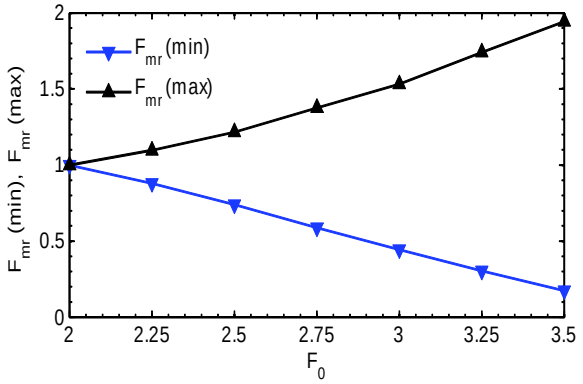

Fig. 4. The maximum and minimum values of moving reference Froude number versus initial Froude number.

Fig. 8, shows the variation of natural logarithm of wave amplitude versus 2π-wave number, k_w, for different values of Froude number. For a given Froude number, the wave amplitude descends in response to an increase in k_w. Conversely, the wave amplitude ascends as the Froude number increases for a given value of k_w.

It was remarked earlier that the linearly unstable conditions of flow are dominated as the Froude number exceeds the limit value F_0=2. In conformance with this fact, the numerical results demonstrate a relatively time invariant wave amplitude for F_0=2 while a substantial decay in wave amplitude is apparent when F_0<2 (Fig. 7). To further illustrate the latter case, the time evolution of free surface is considered in Fig. 9 for F_0=1.5. Under such a condition, the amplitude of initial disturbance would theoretically approach zero if the time goes to infinity. The simulated free surface profiles in Fig. 9 reveal this pattern of amplitude decay and the flow practically recovers its undisturbed steady state at the end of simulation time.

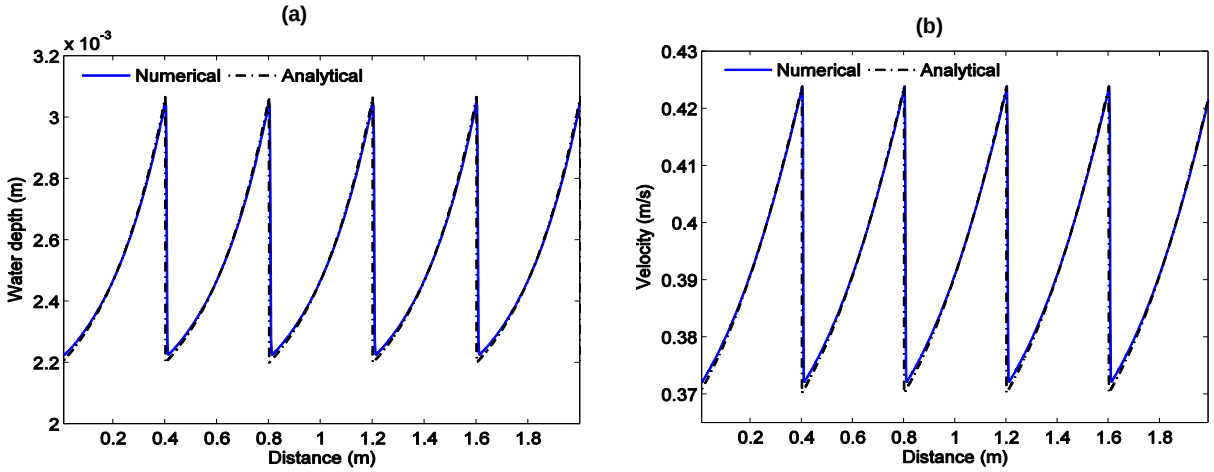

Fig. 5. Comparison between simulated roll waves and analytical solution of Dressler (1949) for a: flow depth and b: flow velocity.

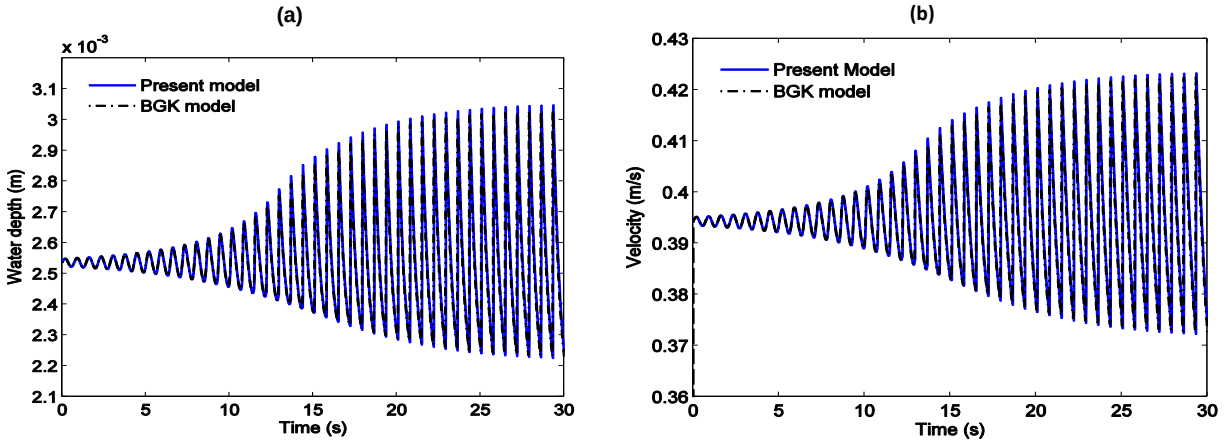

Fig. 6. Time histories of flow variables at the middle of channel ($x = 1\mathrm{m}$) for a: flow depth and b: flow velocity.

Please cite this article as: A. Mahdavi, A TVD-WAF finite volume model for roll wave simulation, Journal of Applied Research in Water and Wastewater, 3 (2), 2016, 241-246.

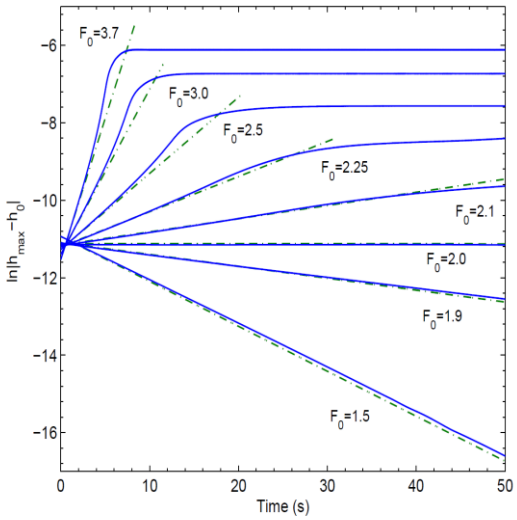

Fig. 7. Time evolution of the natural logarithm of wave amplitude under different Froude numbers and comparison with linear theory (Que and Xu, 2006). (Solid line: Present study; Dash-doted line: linear theory).

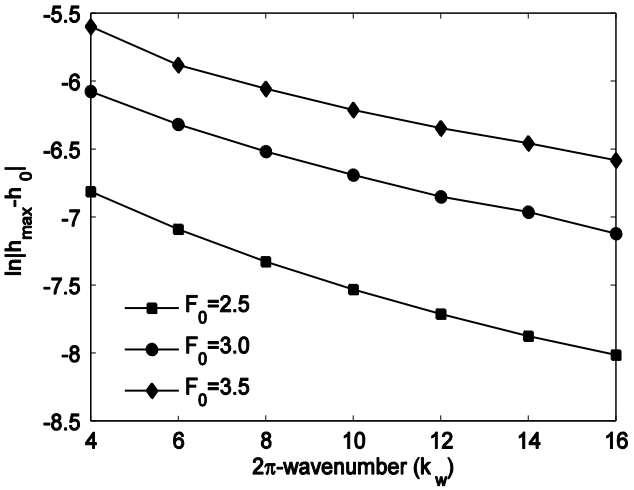

Fig. 8. Natural logarithm of wave amplitude as affected by changes in for different Froude numbers.

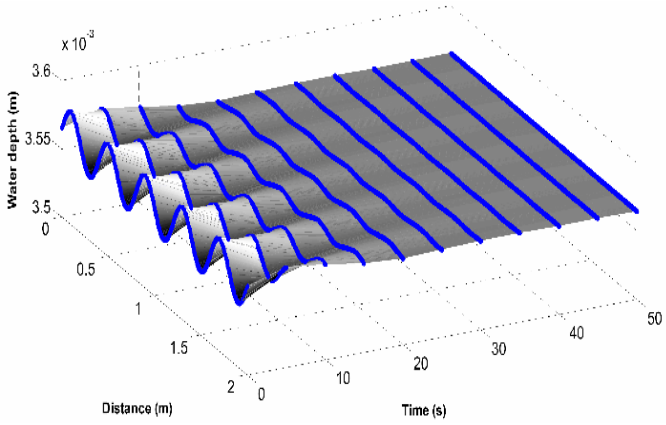

Fig. 9. Temporal decay of initial disturbance for $F_0 = 1.5$.

4. Conclusions

The TVD–WAF scheme has been combined with a three step splitting scheme to numerically solve the conservative form of one dimensional nonlinear shallow water equations. The model was adopted to investigate the generation and evolution of roll waves down an inclined steep channel. It is accomplished by introducing appropriate initial and boundary conditions in the framework of an initial value problem. The numerical results confirm the capabilities of model as a robust tool to eliminate the numerical instabilities due to small water depths usually encountered in roll wave simulation. Moreover, the present model requires a reduced amount of CPU time when compared to that of a high resolution shock capturing scheme. The amplitude growth of emerged roll waves for $F_0 > 2$ together with amplitude decay of initial disturbance for $F_0 < 2$ are simulated by the scheme and compared satisfactorily with a theoretical approach. The present numerical model requires only modest computational effort and, nevertheless, has the ability to handle free surface flows in cases where shocks and smooth profiles are to be considered simultaneously in the computational domain.

Acknowledgment

The author gratefully acknowledges Prof. Kun Xu and Mr. Que Yin-Tik (Mathematics Department; Hong Kong University of Science and Technology) for providing the BGK model source code for the numerical comparison in this study.

References

Balmforth N.J., Mandre S., Dynamics of roll waves, Journal of Fluid Mechanics 514 (2004) 1–33.

Brock R.R., Development of roll waves in open channels, Technical report, W. M. Keck Lab. of Hydraul.and Water Resources, California Institute of Technology, Report KH-R-16 (1967).

Carver S., Sear D., Valentine E., An observation of roll waves in a supraglacial meltwater channel, Harlech Gletscher, East Greenland, Journal of Glacial Archaeology 40 (1994) 75–78.

Cristo C., Iervolino M., Vacca A., Zanuttigh B., Minimum channel length for roll-wave generation, Journal of Hydraulic Research 46 (2008) 73–79.

Dressler R.F., Mathematical solution of the problem of roll waves in inclined channel flows, Communications on Pure and Applied Mathematics 2 (1949) 149–194.

Fer I., Lemmin U., Thorpe S.A., Winter cascading of cold water in Lake Geneva, Journal of Geophysical Research 107 (2003).

Kühne R.D., Macroscopic freeway model for dense traffic-stop-start waves and incident detection, In Proceedings of the 9th International Symposium on Transportation and Traffic Theory (1984) 21–42.

Lukáčová-Medviďová M., Teschke U., Comparison study of some finite volume and finite element methods for the shallow water equations

Please cite this article as: A. Mahdavi, A TVD-WAF finite volume model for roll wave simulation, Journal of Applied Research in Water and Wastewater, 3 (2), 2016, 241-246.

with bottom topography and friction terms, ZAMM - Journal of Applied Mathematics and Mechanics 86 (2006) 874–891.

Mahdavi A., Hashemi M.R.,Talebbeydokhti N., A localized differential quadrature model for moving boundary shallow water flows, Journal of Hydraulic Research 50 (2012) 612–622.

Mahdavi A., Talebbeydokhti, N., Modeling of non-breaking and breaking solitary wave run-up using FORCE-MUSCL scheme Journal of Hydraulic Research 47 (2009) 476–485.

Mahdavi A., Talebbeydokhti N., Modeling of non-breaking and breaking solitary wave run-up using shock-capturing TVD-WAF scheme, KSCE Journal of Civil Engineering, 15 (2011) 945–955.

Montes S., Hydraulics of open channel flow. ASCE Press, USA (1998).

Que Y.-T., Xu K., The numerical study of roll-waves in inclined open channels and solitary wave run-up, International Journal for Numerical Methods in Fluids 50 (2006) 1003–1027.

Toro E.F., Riemann problems and the WAF method for solving the two-dimensional shallow water equations, Philosophical Transactions of the Royal Society A 338 (1992) 43–68.

Toro E.F., Shock-capturing methods for free-surface shallow flows. Wiley, Chichester UK (2001).

Whitham J., Linear and nonlinear waves. Wiley, New York (1974).

Zanuttigh B., Lamberti A., Roll waves simulation using shallow water equations and weighted average flux method, Journal of Hydraulic Research 40 (2002) 610–622.

Zanuttigh B., Lamberti A., Analysis of debris wave development with one-dimensional shallow-water equations, Journal of Hydraulic Engineering 130 (2004) 293–304.

Please cite this article as: A. Mahdavi, A TVD-WAF finite volume model for roll wave simulation, Journal of Applied Research in Water and Wastewater, 3 (2), 2016, 241-246.